Title
Measurement of Thermal Diffusivity and Conductivity in Advanced Nanostructured Materials

Author
Teweldebrhan, Desalegne Bekuretsion

Publication Date
2012

Peer reviewed|Thesis/dissertation

UNIVERSITY OF CALIFORNIA
RIVERSIDE

Measurement of Thermal Diffusivity and Conductivity in Advanced Nanostructured Materials

A Thesis submitted in partial satisfaction
of the requirements for the degree of

Master of Science

in

Materials Science and Engineering

by

Desalegne Bekuretsion Teweldebrhan

March 2012

Thesis Committee:

Dr. Alexander A. Balandin, Chairperson
Dr. Cengiz Ozkan
Dr. Alexander Khitun
Dr. Roger Lake

The Thesis of Desalegne Bekuretsion Teweldebrhan is approved by:

_____

_____

_____

Committee Chairperson

University of California, Riverside

ABSTRACT OF THE THESIS

Measurement of Thermal Diffusivity and Conductivity in Advanced Nanostructured Materials

by

Desalegne Bekuretsion Teweldebrhan

Master of Science, Graduate Program in Materials Science and Engineering
University of California, Riverside, March 2012
Professor Alexander A. Balandin, Chairperson

Continuous device downscaling, growing integration densities of the nanoscale electronics and development of alternative information processing paradigms, such as spintronics, call for drastic increase in the data storage capacity. There is a strong need to engineer alternative materials, which can become foundation of new computational paradigms or lead to other applications such as efficient energy conversion. In this thesis I review results for the thermal and magnetic characterization of the near-field optical transducer for the heat-assisted magnetic recording for beyond the 10-Tbit/in^2 densities. In order to record information, the heat-assisted magnetic recording system uses not only magnetic but also thermal energy. For this reason the recording media with the

substantially higher anisotropy could be utilized to achieve the ultra-high recording densities. The heat-assisted magnetic recording and spintronic information processing require accurate thermal management of magnetic thin films. Here I report the results of the investigation of the thermal transport in Pd/CoPd/Pd magnetic multilayers with the thickness of individual layers in the nanometer range. Also, I investigate the thermal properties of FePt films when deposited on a Ag or Cu heat sink layer with varying thicknesses for the use in heat-assisted magnetic recording. It was found that the FePt films grown on Cu demonstrated the $L1_0$-FePt (001) texture while the FePt films grown on Ag appeared to be isotropic. As the thickness of the heat sink layer increased from 15 to 120 nm, the coercivity of the FePt films decreased from 1.7 – 1.5 Tesla for Cu, and 1.3 – 1.0 Tesla for Ag. Thermal conductivity measurements showed that as Ag and Cu thickness increased, the out-of-plane thermal conductivity decreased, demonstrating that the thermal conductivity can be adjusted by varying the heat sink layer.

Contents

List of Figures

List of Tables

Chapter 1

Introduction

1.1 Motivations

As the roadmap for technology continues to move towards more advanced techniques and improved performance gains, growing limitations continue stress the importants of understanding materials properties typically used for many of modern device components. This is done by producing smaller feature sizes, incorporation of nano-materials, increasing number of transistors per wafer, wafer size growth, and the overall reduction in defect density. Along with its ability to help advance beyond technological expectations, many growing number of challenges begin to arise with each new generation which will need to address.

As an example, with its high performance capacity, silicon-based contemporary metal oxide semiconductor (Si-CMOS) transistor architectures are considered the most common used in today's electronics industry. With a miniaturization process utitilized to

advance this technology, increased heat generation per unit area and increase thermal resistance require that better cooling systems are necessary for further advancements in such technological application. Currently levels of heat generated in processors exceed 100 watts/cm^2, which can be categorized to be on the order, if not greater, than the heat produced from a nuclear reactor as shown in Figure 1.1.

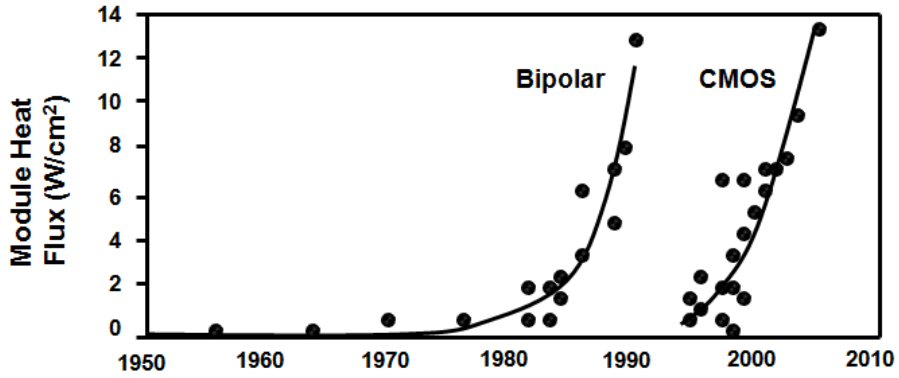

Figure 1.1: Plot indicates the increasing trends of heat produced from different generation of bipolar and CMOS architecture generations.

Traditionally, scaling laws were also followed to advance the data storage industry but in a similar fashion due to the findmental superparamagnetic limit, simple scaling approach cannot be justified and new technology solutions are required. As for silicon based transistors, physical and technological limitations has sparked continuous research towards novel material with extraordinary properties have growingly been important to help meet the demands of the next generation of devices [1]. In the field of material science and disciplines alike, extensive research studies has been devoted into looking at alternative materials for devices integration with current technology.

The transistor is made up of several materials with a variety of physical properties that together allow for fast switching capabilities in the presence of an external field. Traditionally, thin layers of several semiconducting material and high thermal conductivity metal such copper have been used to construct such devices. The aggressive downscaling of the feature sizes and compact integration for new and complex structures continuously requires expensive replacement of tools and instrumentations. With that the technology is being pushed to its limits, standard materials and new materials must both be capable of being processed using state of the art methods for device fabrication. New and innovative ideas are also critical to meet the demands of device miniaturization and patterning techniques. A promising approach has recently been to look at incorporating materials with low dimensionalities that exhibit extraordinary properties into the chip design to help improve the device ability to perform effectively.

1.2 Thermal Properties

Theoretical predictions have been made by several researchers [2-4], regarding significant change in thermal properties of quantum well structures owing to the spatial confinement of charge carriers and the resultant change in carrier density of states. These reports however ignored the effects of spatial confinement and bulk values of thermal conductivity were used. The total thermal conductivity in semiconductor materials can be expressed as a sum of two components

$$K = K_l + K_e \qquad [1.1]$$

where K is the total thermal conductivity, K_l is the component due to lattice vibrations and K_e is the component due to electrical charge carriers. These vibrations are not perfectly elastic, since the elastic modulus varies from point to point according to the displacement of the atoms from their equilibrium positions.

1.2.1 Phonons

When atoms are displaced this gives rise to scattering of vibrational waves [3-4] and phonon wave packets originate from these waves. It can be thought of as a collective vibration of the whole system and not individual atoms. The vibration of the whole system can be broken down into normal modes of lattice vibration. As photons are the quanta of electromagnetic field, phonons act as the quanta of excitation of normal modes of vibration. These phonons normally propagate through a perfectly elastic crystal without interfering with one another, but at high temperature due to Umklapp process, momentum is not conserved in the phonon- phonon interaction and this introduces thermal resistance and the thermal conductivity is limited and varies as 1/T. In a metal, conduction electrons are responsible for the transport of both heat and charge. The lattice part of the thermal conductivity is usually negligible in a metal, firstly because of the scattering of phonons by the electrons, and secondly because the electron component K_e is so great. The doped extrinsic semiconductors have very high 8 electrical conductivity and the conduction of heat is mostly due to lattice vibrations and phonons are the primary heat carriers. Whenever there is a temperature gradient, phonon distribution shifts from

its equilibrium value. The various mechanisms of phonon scattering tend to bring back the system to equilibrium.

1.3 Confined Nanostructures

As a result of spatial confinement, it is been shown that classical physics breaks down and new effects can modify a material's properties. For example, in confined structures it has been theoretically shown that modification to a material's density of state occurs which directly affect how the material interacts with electrons, point defects, phonons, etc. As a benefit, in some cased low-dimensional confinement may also be utilized to enhance some material properties and allow for increased functionality e.g. electronic band gap tuning. Typically, one would need to produce nanostructures with thickness shorter than de Broglie wavelength of the material, typically less than 100nm in feature size.

$$\lambda = \frac{h}{p} \qquad\qquad p = \frac{E}{c} \qquad [1.2]$$

1.3.1 Quantum Wells

It has been theoretically predicted that atomically thin films metals and semimetals are thermodynamically unstable, and none could be shown to exhibit any notable field effect. Theoretical predictions have also projected that significant change in the thermal properties of quantum well structures is possibly due to the confinement of

charge carriers, which results in change to the carrier density of states [3]. These reports however ignored the effects of spatial confinement of phonons and bulk values of thermal conductivity were used. The spatial confinement of phonons in nanostructures and thin films can affect the phonon dispersion strongly and modify phonon properties such as phonon group velocity, polarization, and the interaction of phonons with other particles [2]. Such altered affects in quantum wells is only possible if materials are crystalline and essentially free of defects. The thickness of the thin film required to achieve the quantum confinement conditions has to be on the order of few atomic layers. Superlattices, which are commonly used for confined wells, are only partially confined with small potential barrier height and of relatively low material quality.

The phonon transport and hence the lattice thermal conductivity of superlattices depend on miniband formation and a new kind of Umklapp scattering process called mini- Umklapp process. This is related to the transition between the mini Brillouin zone of the superlattice [5]. These superlattices had alternate layers of insulators in between and the phonon transport was altered by the periodicity in the direction of layering. Along this particular direction, the alternating layers of crystal lattice give rise to mini Brillouin zones. The mini reciprocal lattice vectors associated with these mini zones give rise to mini Umklapp scattering which contribute to the thermal resistance [6]. Total internal refection confines the phonon modes in the superlattice and reduces the group velocity of phonons significantly. At high temperatures, this acoustic mismatch causes a reduction in superlattice thermal conductivity by one order of magnitude.

If the quantum well structures have boundaries which have similar elastic and crystalline properties as the structures themselves, then the 11 phonon modes would extend thorough the boundaries. The case would be then quite similar to a bulk material. However, if the quantum well structures are free standing or embedded in rigid materials with markedly different elastic properties, the story would be entirely different as has been shown in [2]. The phonon confinement effect has a strong influence on phonon relaxation rates and this in turn modifies the group velocity. The thermal transport is thus different from bulk properties. Spatial confinement of phonons in nanostructures and thin films can affect the phonon dispersion strongly and modify phonon properties such as phonon group velocity, polarization etc and influence the interaction of phonons with other particles. In another work [3], thermal transport in one dimensional conductor or quantum wires were studied. Electrons are confined to move in single dimension, parallel to the wire but phonons tend to move in three dimensions and are hence scattered from the surface. This reduces the lattice thermal conductivity strongly.

References

[1] G.E. Moore, "*Cramming More Components onto Integrated Circuits*", *Proc. IEEE*, **86**, 1, 82-85 (1998).

[2] A.A. Balandin, K.L. Wang, K.L., *Journal of Applied Physics*, **84**, 6149 (2008).

[3] L.D. Hicks, and M.S. Dresselhaus, *Physical Review B*, **47**, 16631 (1993).

[4] K.E. Goodson, and Y.S. Ju, *Annual Review of Materials Science*, **29**, 261 (1999).

[5] S.Y. Ren, and J.D. Dow, *Physical Review B*, **25**, 3750 (1982).

[6] A.A. Balandin, *Phys. Low-Dim. Structures*, **0.5**, 1 (2000).

Chapter 2

Experimental Setup

This chapter focuses on the initial processes that were developed for synthesis and methods for experimental analysis of nanostructured materials for data storage technology. Here I start with a simple overview of some of these preparational methods and analysis techniques, and in the following chapter the experimental results will be discussed for the intrinsic thermal properties of magnetic films using Laser-Flash method.

2.1 Laser-Flash Measurement Method

The measurement of the thermal diffusivity of a material is usually performed by rapidly heating one side of a sample and measuring the temperature rise as a function of time on the opposite side of the sample. The recorded time that takes for the heat to travel through the sample and cause the temperature rise on the rear face is used to determine the through-plane diffusivity and calculate the thermal conductivity is the specific heat is know and mass density of the material are known [1]. Using a Netzsch

LFA 447 Nano-flash system, we are able to compare thermal trends for samples. In these measurements a xenon-flash-lamp laser is used to produce shots of 10J/pulse to one end of the sample surface, while temperature rise is measured on the other end using a nitrogen-cooled indium antimonide (InSb) infared detector. Laser-flash technique (LFT) is a contactless method used to measure the traveling time of the thermal wave excited from that of a high intensity short duration light pulse, which is used to evaluate the thermal diffusivity (α).

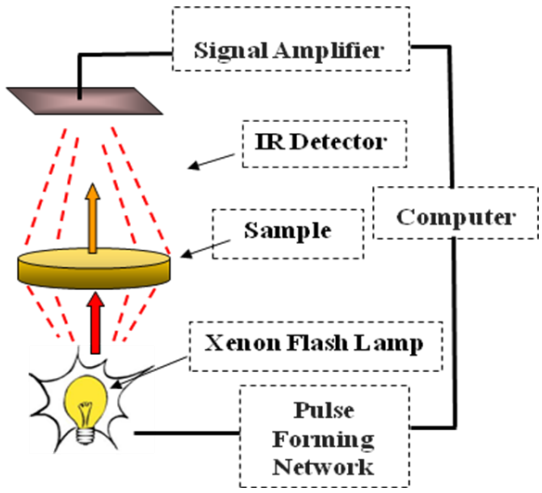

Figure 2.1: Schematic of the experimental setup used for measurement of the thermal diffusivity of the magnetic recording media. The "laser flash" type of measurement is based on illumination of the one side of the sample and detecting the temperature rise with IR detector on the opposite side of the sample.

Assessment of measured data were done using radiation and pulse correction along with the half-time method of temperature rise pulses with $\alpha=0.1388*(d^2/t_{1/2})$, where d is sample thickness and $t_{1/2}$ is the pulse half rise time, respectively [1]. The thermal conductivity is determined as $K= \alpha\rho C$, where ρ and C correspond to the mass density and

specific heat of the material, respectively. For layered thin film material, depending on the dimentionality of the sample, both inplane and cross-plane thermal characteristics maybe looked at in thin films [2,3]. Using the Netzsch LFA system, we begin by calibrating the instrument by accurately measuring materials with know thermal properties. In Figure 1.2, varies plots show thermal conductivity (*K*) values for different forms of silicon and silica (SiO_2) measured. Unlike crystslline bulk silicon, a gradual increase in *K* value with *T* is characteristic for the disordered materials.

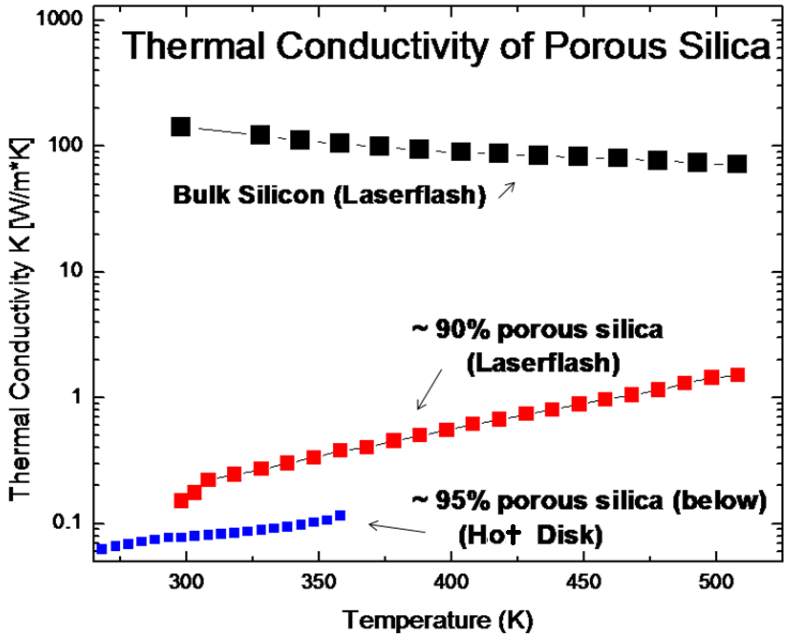

Figure 2.2: Plots show thermal conductivity (*K*) values for different forms of silicon and silica (SiO_2) measured.

2.2 Hot Disk Method

Thermal conductivity measurements are also carried out with a TPS technique called hot disk, for confimationa and comparison as well. The noncontact optical LFT

approach works better for films and is processed several times to make sure systematic error is within acceptable limits. Shot pulses are carefully processed to meet, for accurate extraction of thermal diffusivity and accurate modeling for thermal conductivity measurements. For this work measurements were investigated with two distinctively different experimental techniques, a transient planar source (TPS) technique, known as the hot-disk method, and an optical laser flash technique (LFT). Both experimental techniques are utilized as extraction methods for extracting the thermal properties of bismuth telluride layered films. For hot disk technique, a Ni based thin spiral heater/sensor, coated with an electrically insulating Kapton layer, is then placed between two thin layered films of equal thickness. As a result of temperature rise, the sensor determines from the change in the resistance from the dissipated heat along the in-plane direction of our thin structures. The thermal conductivity extractions for these samples are observed from temperature rise:

$$\overline{\Delta T(\tau)} = P(\pi^{3/2} rK)^{-1} D(\tau)$$

where τ is the parameter related to the thermal diffusivity α and the transient measurement time t_m through the expression $\tau = \left(t_m \alpha / r^2\right)^{1/2}$, r is the radius of the sensor, P is the input power for heating the sample, and $D(\tau)$ is the modified Bessel function [4,5].

References

[1] W.J. Parker, R.J. Jenkins, C.P. Butler, and G.L. Abbott, *J. Appl. Phys*., **32**, 1679 (1961).

[2] L. Kehoe, P. V. Kelly, and G.M. Crean, *Microsystem Technologies,* **5**, 18 (1998).

[3] V. Goyal, D. Teweldebrhan, and A.A. Balandin, *Appl. Phys. Lett.,* 133117 (2010).

[4] E. Silas Gustafsson, Silas E., *Review of Scientific Instruments*, **62**, 797 (1991).

[5] M. Gustavsson , E. Karawacki , and E. Silas Gustafsson., *Review of Scientific Instruments*, **65**, 3856 (1994).

Chapter 3

Heat-Assisted Magnetic Recording Nanomaterials

3.1 Motivation for Thermal Cooling in Magnetic Materials

Heat-assisted magnetic recording (HAMR) has been considered a potential method of increasing the areal density beyond the limitations of conventional perpendicular magnetic memory recording [1,2]. In HAMR, the recording media is heated near its Curie temperature during the writing process and needs to cool down quickly to avoid thermal destabilization of adjacent tracks. Furthermore, the bit transition length depends on the thermal gradient of the media as well as the magnetic field gradient. Also, the high temperatures associated with HAMR can affect other aspects of the device. Therefore, a rapid cooling rate is critical to achieve a sharp bit transition. This leads to an important trade-off between fast heating and rapid cooling, which can be tuned with the use of a heat sink layer.

Conventional magnetic recording schemes are coming to their end because of the superparamagnetic limit [3], but heat-assisted magnetic recording (HAMR) may have potential to extend the data densities to 10 Terabit/in^2 [4-7]. In order to record information, HAMR will use not only magnetic but also thermal energy. Therefore, a recording media with substantially higher anisotropy could be utilized. In one of the proposed implementations, a laser beam in the near field, co-aligned with the recording field, heats up a local region to the temperature close to the Curie point. The key challenge in this implementation is to develop a near-field transducer capable of delivering over 50 μW into a spot diameter of 30 nm.

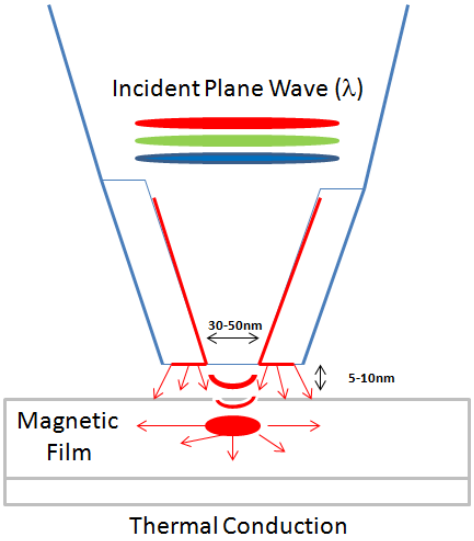

Figure 3.1: Schematic of the cross-section of NSOM probe depicting the heat sources and thermal conduction paths.

The traditional fiber schemes are barely capable of producing 10 nW. To resolve this issue, a laser diode could be placed with the emitting edge only a few nanometers away

from the recording media. The light can propagate through a nano-aperture on the surface of an aluminum-coated emitting edge.

3.2 Experimental Setup

In this section we present an overview of our recent experimental studies focused on recording characteristics of the various near-field transducers fabricated using the focused ion beam (FIB) technology [8]. In order to count the number of photons emitted in the near field we have implemented a special near-field scanning optical microscopy (NSOM) system (see Figure 3.1). Here FIB-fabricated transducers could deliver power of over 100 nW into a 35-nm spot. The heat assisted magnetic recording requires precise control of the heat propagation in the recording medium and accurate thermal management of the whole system. In this work we address the thermal management issues and present preliminary results of the thermal conductivity measurements using the nano-flash technique.

3.2.1 Thermal Diffusivity of Layered Magnetic Media

The heat assisted magnetic recording requires accurate knowledge of the thermal diffusivity α and thermal conductivity K of the materials used as recording medium as well as NSOM probe materials. Transient heat transfer occurs when the temperature distribution or heating source power are changing with time. The fundamental quantity that describes the heat transfer when the system is not at steady-state is the thermal diffusivity α. The thermal diffusivity is related to thermal conductivity through the expression $\alpha=K/\rho C_p$, where ρ is the mass density and C_p is the specific heat of the

material. In this section we give an overview of our preliminary results of the thermal characterization. The long term goal of the study of the thermal diffusivity and thermal conductivity described here is to improve the thermal management of the HAMR systems and develop an optimum NSOM design within the thermal constrains.

The measurement of the thermal diffusivity of a material is usually performed by rapidly heating one side of a sample and measuring the temperature rise as a function of time on the opposite side of the sample (see Figure 2.1). The recorded time that takes for the heat to travel through the sample and cause the temperature rise on the rear face is used to determine the through-plane diffusivity and calculate the thermal conductivity is the specific heat is know and mass density of the material are known. The Netzsch system, which we used for this study, allows measurements of thermal diffusivity values ranging from 0.001 to 10 cm^2/s over a temperature range from 20^{o}C to 160^{o}C.

3.3 Thermal Properties of Pd/CoPd/Pd Multilayers

The magnetic recording media, which consists of Pd/CoPd/Pd multilayers, were prepared on the Corning 0211 glass substrates (Zinc Borosilicate). The total thickness of the multilayers varied from approximately 30 to 65nm. The first essential step was to accurately determine the thermal diffusivity and thermal conductivity of the substrates used. This is required in order to be able to separate the value of the thermal diffusivity for the thin multilayers from that of the substrate. Figure 3.2 shows the measured thermal diffusivity for the Corning 0211 substrate as a function of temperature. As one can see from this plot the room-temperature value is α=4.27×10^{-7} m^2/s.

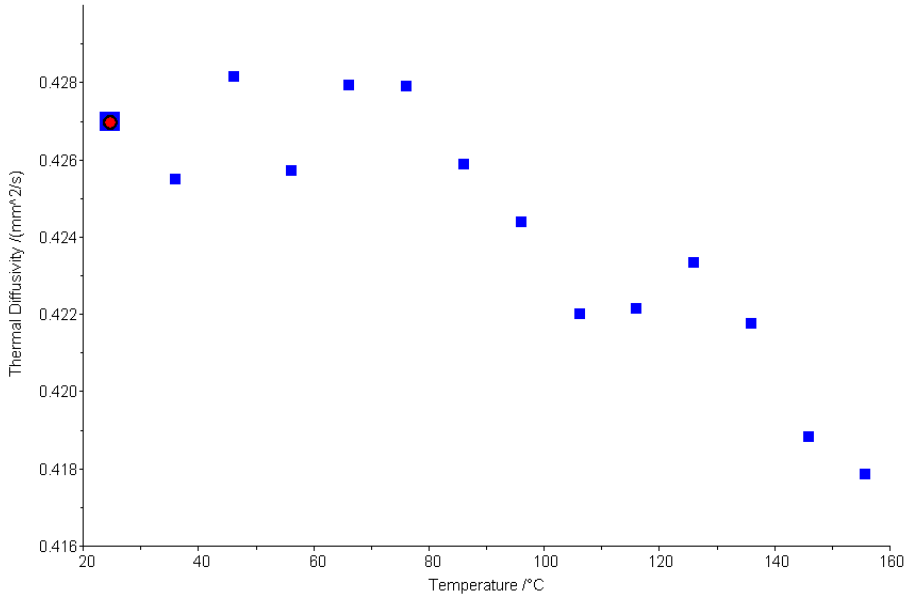

Figure 3.2: Measured thermal diffusivity of the substrate used for Pd/CoPd/Pd multilayer deposition.

The measured value and temperature dependence are in excellent agreement with the data reported in literature for glass. For example, in Ref. [9], the thermal diffusivity of glass, measured using the photopyroelectric signal spectral analysis, was determined to be ~4.3×10^{-7} m^2/s at room temperature. It also manifested decreasing trend as the temperature increased from 100K to 300K [9]. The agreement with the previously published data indicates that our experimental technique is accurate and fits well the samples of given geometry and material composition. Using a reference sample with the known temperature dependence of specific heat we were able to determine the thermal conductivity of the Corning 0211 substrates (see Figure 3.3). The determined thermal

conductivity increases with temperature as typical for the amorphous bulk materials or disordered alloys [10-12].

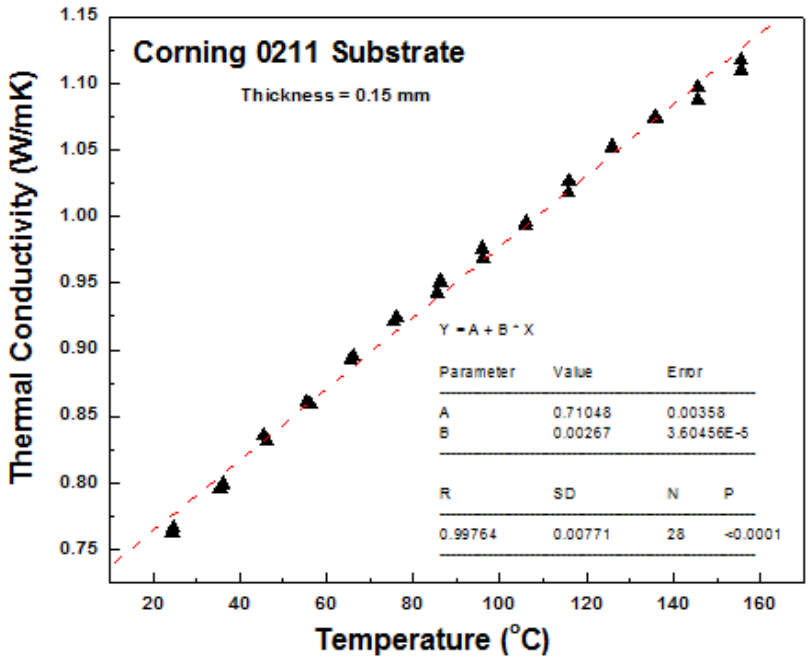

Figure 3.3: Measured thermal conductivity of the substrate used for Pd/CoPd/Pd multilayer deposition.

After the thermal diffusivity and thermal conductivity values for the substrates have been determined, we focused on the study of Pd/CoPd/Pd multilayers deposited on the Corning 0211 substrates. The thermal diffusivity data for the multilayers revealed much more scatter as compared to the substrate data. Table I gives a summary of the room-temperature results obtained for several samples of different thickness. The diffusivity values were extracted using the adiabatic model with the pulse correction.

Sample Type	Pd/CoPd/Pd	Pd/CoPd/Pd/CoPd/Pd	Pd/CoPd/Pd/CoPd/Pd
Thickness (nm)	40	63	63
α, $\times 10^{-6}$ (m^2/s)	10.0	1.1	0.83

Table I: Measured Thermal Diffusivity of the Pd/CoPd/Pd Multilayers

Although there have been no previous studies of the thermal diffusivity in such magnetic multilayers it is interesting to compare the obtained results with the previously reported data for Pd and other related alloys. The photoacoustic measurements of the thermal diffusivity of Fe-Co-Al alloys revealed the value of ~ 11.4 $\times 10^{-6}$ m^2/s for $Fe_{0.45}Co_{0.1}Al_{0.45}$ [13]. The α value for this alloy was much smaller than the values of the constituent elements, which are 22.7 $\times 10^{-6}$, 26.8 $\times 10^{-6}$, and 97.9 $\times 10^{-6}$ m^2/s for Fe, Co and Al, respectively [13]. In another study the room-temperature thermal diffusivity of the Ag-Pd alloys was found to be in the range from 10.8 $\times 10^{-6}$ to 23.1 $\times 10^{-6}$ m^2/s, which was also smaller than the thermal diffusivity of pure Pd of 24.7 $\times 10^{-6}$ m^2/s [14].

The data, which we measured for the Pd/CoPd/Pd multilayers is consistent with the previous studies of alloys containing Pd and Co. We also observed a decrease in the thermal diffusivity of the multilayers as compared to the thermal diffusivity of Pd (α=24.7 $\times 10^{-6}$ m^2/s) and Co (α=26.8 $\times 10^{-6}$ m^2/s) metals. There are two possible effects, which lead to the thermal diffusivity and thermal conductivity reduction. It is well known that heat in metals and alloys is carried by both electrons and acoustic phonons [11]. The increase acoustic phonon scattering in alloys can result in substantial reduction of the

phonon thermal conductivity as was found for many materials [15]. Electrons can also be scattered by the alloy disorder with corresponding decrease in thermal conductivity. In addition, the reduction of the thermal diffusivity can be the result of the thermal boundary resistance (TBR) also referred to as Kapitza resistance [16]. The Kapitza resistance at the interface between two solid materials can be rather large even at room temperature [17]. The fact that the thermal diffusivity for the samples with the 63-nm thickness (which have more different layers) was stronger than that for the samples with 40-nm thickness supports an assumption about strong TBR effect.

Our thermal study revealed that the thermal properties of the nanometer scale multilayers are different from the thermal properties of constituent elements and conventional random PdCo alloys. Even further deviation in properties is expected as the individual layer thickness decreases further. In this case, one may expect the acoustic phonon confinement effects [18] and altered electron – phonon interaction. The latter deserves a separate study. The accurate values of the thermal diffusivity and thermal conductivity can be used in the thermal design optimization of the layered magnetic recording medium for the HAMR systems considered in this paper, multilevel three-dimensional nanomagnetic recording media [19-20] and spin logic circuits implemented on the basis of Ni-Fe alloy thin films on semi-insulating substrates [21].

3.4 Comparative Heat Sinks in $L1_0$-FePt HAMR Thin Films

$L1_0$-FePt thin films are a promising candidate for HAMR media due to its high magnetic anisotropy [22]. For a heat sink layer to be incorporated into FePt HAMR

media, the material should demonstrate high thermal stability as well as a compatible crystalline structure for $L1_0$-FePt. Both Ag and Cu are well-known as heat sink materials in electronic devices due to their high thermal conductivity of 430 and 400 W/m K, respectively. They also display a low coeffecient of thermal expansion. Also, studies have shown that Ag and Cu have similar crystal structures when sputter deposited [23]. In this work, FePt thin films were grown on both Ag and Cu underlayers to study their feasibiltiy as heat sink materials. The structure and magnetic properties were investigated, as well as the out-of-plane thermal conductivity of the FePt thin films.

3.4.1 $L1_0$-FePt Nanostructure Characterization

The structure of the films was Si/Ag or Cu/Ta (2 nm)/CrRu (25 nm)/MgO (2 nm)/FePt (5nm) prepared by rf (MgO layer) or dc (all other layers) magnetron sputtering. The Ag and Cu heat sink layers were deposited at room temperature with 3 mTorr sputter pressure. The thickness of the heat sink layer was varied at 15, 30, 60, and 120 nm. The Ta layer was deposited at room temperature with a sputter pressure of 10 mTorr, while the CrRu layer was deposited at 300 °C using 3 mTorr sputter pressure. The samples were cooled to room temperature before depositing the MgO layer at 90 °C and the FePt layer at 550 °C, with 5 mTorr and 10 mTorr pressure, respectively. The crystal structure of the films was measured by x-ray diffraction (XRD) while the magnetic properties were measured by a room temperature magneto-optical Kerr effect (MOKE) with an applied field of ± 2.7 Tesla. The thermal conductivity (K) was measured by a laser-flash technique, where a xenon light source produces a pulse at the surface of the sample, while an InSb infared detector measures the temperature rise on the opposite side. This

directly measures the out-of-plane thermal diffusivity (α) through the FePt thin films on Si substrate, then by using the sample's specific heat (C_p) and mass density (ρ) allows for calculation for the thermal conductivity (K) of layered sample ($K=\rho\alpha C_p$).

3.4.2 Results and Discussion

Figures 1 and 2 show the XRD patterns of the FePt thin films grown on Ag [Fig. 1] and Cu [Fig. 2] layers with thicknesses of (a) 15, (b) 30, (c) 60, and (d) 120 nm. None of the samples grown on the Ag layer exhibited FePt (001) texture, while all samples grown on the Cu layer showed preferred $L1_0$-FePt (001) texture. This is attributed to the fact that the CrRu (002) texture is not formed on the Ag layer, which is necessary to grow FePt (001) perpendicular orientation. Also of note, the samples grown on Ag do not exhibit FePt(111) texture, demonstrating that the FePt films grown on Ag are not perpendicullary oriented nor longitudinally oriented.

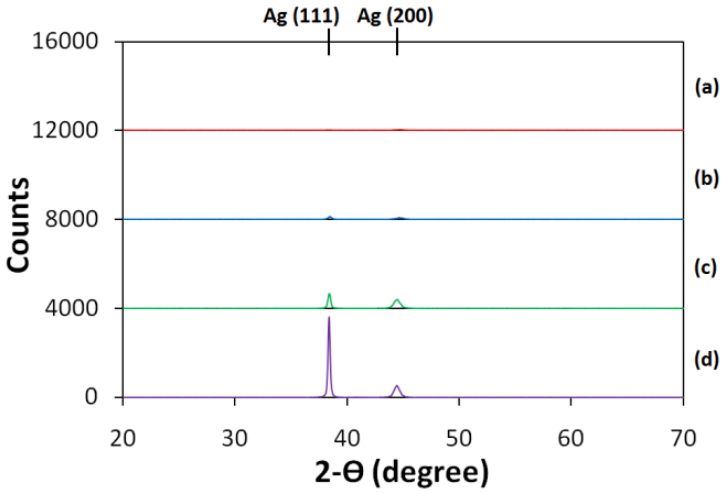

Figure 3.4: XRD spectra of FePt thin films grown on a Ag heat sink layer of (a) 15 nm, (b) 30 nm, (c) 60 nm, and (d) 120 nm.

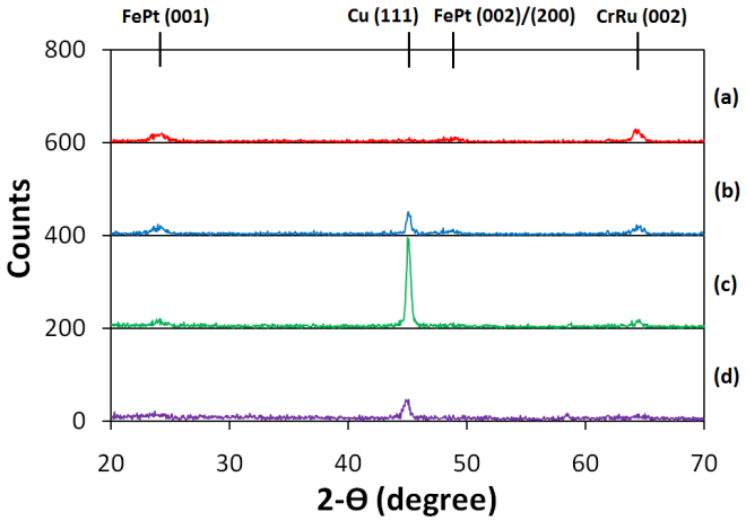

Figure 3.5: XRD spectra of FePt thin films grown on a Cu heat sink layer of (a) 15 nm, (b) 30 nm, (c) 60 nm, and (d) 120 nm.

The out-of-plane hysteresis loops of the FePt films grown on Ag and Cu layers with varying thicknesses. In both cases, the coercivity of the FePt films decreases as the thickness of the heat sink layer increases. For the FePt films grown on Ag, the coercivity decreases from 1.3 – 1.0 Tesla, while the coercivity decreases from 1.7 – 1.5 Tesla for the FePt films grown on Cu. For the samples grown on Cu, this decrease in coercivity can be attributed to the fact that as the thickness of the Cu layer inreases, both the CrRu (002) and FePt (001) XRD peaks decrease, as seen in Figure 3.5. By varying the thickness of the heat sink layer, the thermal properties of the FePt films can be adjusted so that media can be heated quickly to its Curie temperature, but also cooled fast enough to avoid thermal erasure of adjacent tracks.

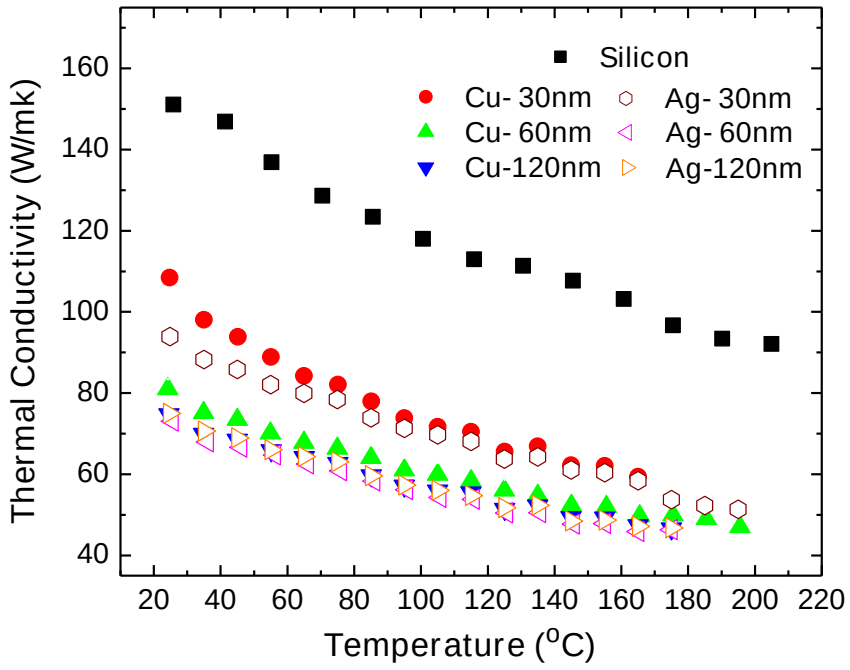

Figure 3.6: Out of plane thermal conductivity of FePt thin films grown on Ag and Cu heat sink layers of varying thicknesses.

In Figure 3.6 it is shown the thermal conductivity vs. temperature of the FePt films grown on Ag and Cu layers of 30nm, 60nm and 120 nm thicknesses. A bulk crystalline Si substrate was also measured for comparison. Since the sample is heated on the surface (FePt layer) but the temperature rise is measured at the opposite side (Si substrate) it is expected that the thermal conductivity for all the samples would decrease due to scattering at the layered interfaces as compared to the bulk crystalline Si substrate. This is because the thermal conductivity is measured in the out-of-plane vertical direction of the layered sample, so that when the FePt films are deposited, some of the heat is dissipated in the horizontal direction, resulting in less heat measured at the bottom end of

the sample. Thermal boundary resistance (TBR) also may result in lowering of thermal transport as a result of interface scattering. Here we neglect such TBR effects as slight variation of the thickness of heat sink layer has larger effect on measurements. Here we show as the thickness of the heat sink layer increases, the thermal conductivity decreases, showing that more and more heat is being dissipated horizontally through the heat sink layer. Similar planar integration of high thermal conductivity materials for heat management techniques have recently been proposed for thin carbon-based materials [24, 25]. This is especially true for Cu, where the sample with a 30 nm Cu layer shows much higher thermal conductivity than the other samples. Thus, it can be determined that the thermal properties of the FePt films can be tuned cool faster or slower if desired.

References

[1] M. A. Seigler, W. A. Challener, E. Gage, N. Gokemeijer, G. Ju, B. Lu, K. Pelhos, C. Peng, R. E. Rottmayer, X. Yang, H. Zhou, and T. Rausch, *IEEE Trans. Magn.* **44**, 119 (2008).

[2] M. H. Kryder, E. C. Gage, T. W. McDaniel, W. A. Challener, R. E. Rottmayer, G. Ju, Y.-T. Hsia, and M. F. Erden, *Proceed. IEEE* **96**, 1810 (2008).

[3] Dieter Weller and Andreas Moser, *IEEE Transactions on Magnetics*, **35**, 6, (1999).

[4] K. Matsumoto, A. Inomata, S. Hasegawa, *FUJITSU Sci. Tech. J.*, **42**,1, 158, (2006).

[5] Hendrik F. Hamann, Yves C. Martin, and H. Kumar Wickramasingheb, *Appl. Phys. Lett.*, **84**, 52, (2004).

[6] Hiroyuki Katayama, Masaki Hamamoto, Jun-ichi Sato, Yoshiteru Murakami, and Kunio Kojima, *IEEE Transactions on Magnetics*, **36**, 1 (2000).

[7] T. McDaniel and W. Challener, *IEEE Transactions on Magnetics*, **39**, 1972 (2003).

[8] S. Khizroev and D. Litvinov, *Review in Nanotechnology*, **14**, R7-15 (2004).

[9] B. Bonno, J.L. Laporte and R. Tascon d'Leon, *Rev. Sci. Instrum*., **67**, 3616 (1996).

[10] M. Shamsa, W.L. Liu, A. A. Balandin, C. Casiraghi, W.I. Milne, A.C. Ferrari, *Appl. Phys. Lett.* 89, 161921 (2006).

[11] A.A. Balandin, *Thermal conductivity of semiconductor nanostructures, in Encyclopedia of Nanoscience and Nanotechnology* edited by H.S. Nalwa, 425 (2004).

[12] M. Shamsa, W.L. Liu, A.A. Balandin and J.L. Liu, *Appl. Phys. Lett*., **87**, 202105 (2005).

[13] K.A. Azez, *J. Alloys and Compounds*, **424**, 4 (2006).

[14] K. Miyanaga, Y. Kayano and H. Inoue, *IEICE Trans. Electron*., **E90-C**, 1405 (2007).

[15] W. L. Liu and A. A. Balandin, *Appl. Phys. Lett*., **85**, 5230 (2004); W.L. Liu and A.A. Balandin, *J. Appl. Phys.*, **97**, 073710 (2005).

[16] P. L. Kapitza, *Journal of Physics* (Moscow) **4**, 181 (1941).

[17] K. Filippov and A.A. Balandin, *J. Nitride Semiconductor Research*, **8**, 4 (2003).

[18] A. Balandin and K.L. Wang, *Phys. Rev. B*, **58**, 1544 (1998); J. Zou and A.A. Balandin, *J. Appl. Phys*., **89**, 2932 (2001); E.P. Pokatilov, D. Nika and A.A. Balandin, *J. Appl. Phys*., **95**, 5626 (2004); A.A. Balandin, E.P. Pokatilov and D.L. Nika, *J. Nanoelectronics and Optoelectronics*, **2**, 140 (2007).

[19] N. Amos, R. Ikkawi, A. Krichevsky, R. Fernandez, E. Stefanescu, I. Dumer, D. Litvinov and S. Khizroev, *J. Nanoelectron. Optoelectron*., **2**, 257 (2007).

[20] N. Amos, A. Lavrenov, R. Ikkawi, P. Gomez, F. Candocia, R. Chomko, D. Litvinov and S. Khizroev, *J. Nanoelectron. Optoelectron.*, **2**, 202 (2007).

[21] A. Khitun and K.L. Wang, *J. Nanoelectron. Optoelectron.*, **1**, 71 (2006).

[22] D. Weller, A. Moser, L. Folks, M. E. Best, W. Lee, M. F. Toney, M. Schwickert, J.-U. Thiele, and M. F. Doerner, *IEEE Trans. Magn*. **36**, 10 (2000).

[23] A. Zendehnam, M. Ghanati, and M. Mirzaei, *J. Phys.: Conf. Series*, **61**, 1322 (2007).

[24] A. A. Balandin, S. Ghosh, W. Bao, I. Calizo, D. Teweldebrhan, F. Miao, and C. N. Lau, *Nano Lett.*, **8**, 902 (2008).

[25] V. Goyal, S. Subrina, D. L. Nika, and A. A. Balandin, *Appl. Phys. Lett*,. **97**, 031904 (2010).

Chapter 4

Concluding Remarks

It's presented here a look at how alternative material from with integration densities of the nanoscale can be utilized in the development of alternative information processing paradigms which call for drastic increase in the data storage capacity. I have presented results for the thermal and magnetic characterization of the near-field optical transducer for the heat-assisted magnetic recording for beyond the 10-Tbit/in^2 densities. In order to record information, the heat-assisted magnetic recording system uses not only magnetic but also thermal energy. For this reason the recording media with the substantially higher anisotropy could be utilized to achieve the ultra-high recording densities. The heat-assisted magnetic recording and spintronic information processing require accurate thermal management of magnetic thin films. Here I reported results of the investigation

of the thermal transport in Pd/CoPd/Pd magnetic multilayers with the thickness of individual layers in the nanometer range. Also, I show that the thermal properties of FePt films when deposited on a Ag or Cu heat sink layer with varying thicknesses for the use in heat-assisted magnetic recording. It's shown that the FePt films grown on Cu demonstrated the $L1_0$-FePt (001) texture while the FePt films grown on Ag appeared to be isotropic. As the thickness of the heat sink layer increased from 15 to 120 nm, the coercivity of the FePt films decreased from 1.7 – 1.5 Tesla for Cu, and 1.3 – 1.0 Tesla for Ag. Thermal conductivity measurements showed that as Ag and Cu thickness increased, the out-of-plane thermal conductivity decreased, demonstrating that the thermal conductivity can be adjusted by varying the heat sink layer.